

Molecular Complex of Fullerene C₇₀ with a Trinuclear Coordination Assembly of Manganese(II) Tetraphenylporphyrins with OctaazacryptandDmitri V. Konarev,^{*,†} Salavat S. Khasanov,[‡] and Rimma N. Lyubovskaya[†][†]Institute of Problems of Chemical Physics RAS, Chernogolovka, Moscow Region 142432, Russia, and[‡]Institute of Solid State Physics RAS, Chernogolovka, Moscow Region, 142432, Russia

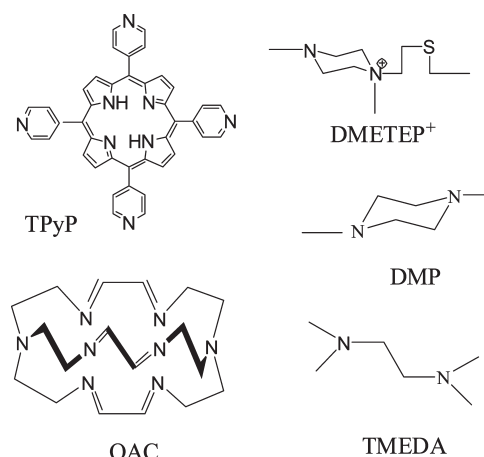
Received July 31, 2009; Revised Manuscript Received February 19, 2010

ABSTRACT: Trinuclear coordination assembly of manganese(II) tetraphenylporphyrins with octaazacryptand (OAC) was obtained for the first time in the complex with fullerene C₇₀: {(Mn^{II}TPP)₃·OAC}·(C₇₀)₃·(C₆H₄Cl₂)₃ (**1**). The Mn^{II}TPP coordinates to imine nitrogen atoms of OAC with the Mn^{II}···N(OAC) distance of 2.283(10) Å. The Mn^{II} atoms deviate by 0.507 Å from the plane of four porphyrin nitrogens toward OAC, providing the concave porphyrin surface, which conforms well to the elongated C₇₀ sphere. Optical data indicate the molecular ground state of the complex. The averaged Mn^{II}···N(TPP) bond length of 2.126(4) Å corresponds to the high-spin (*S* = 5/2) state of Mn^{II}TPP. That was proved by the EPR spectrum of **1**.

For the past few years, essential efforts were made to build organized self-assembled coordination assemblies of metalloporphyrins as possible microporous materials, components for artificial photosynthesis, and solar cells.^{1–8} An interesting peculiarity of these assemblies is their ability to form complexes with fullerenes.^{9–15} By now, fullerene complexes with the coordination assemblies of zinc tetraphenylporphyrin (ZnTPP) were mainly obtained. Among them there are mononuclear structures with pyridine⁹ and tetramethylethylenediamine (TMEDA),¹⁰ binuclear structures with pyrazine,^{10,11} 4,4'-bipyridine (BPy),¹⁰ *N,N'*-dimethylpiperazine (DMP),¹² and a tetranuclear structure with tetra(4-pyridyl)porphyrin (TPyP)^{10,13} (Chart 1). Zinc octaethylporphyrin (ZnOEP) forms a mononuclear structure with diazabicyclooctane and a binuclear structure with BPy, which were also cocrystallized with C₆₀.^{14,15} Fullerene complexes with coordination porphyrin assemblies are interesting not only due to their unusual crystal structures but as possible photoactive compounds and precursors for the synthesis of ionic complexes. For example, it was shown that coordination assemblies of TPyP with ZnTPP or ruthenium tetraphenylporphyrin carbonyl (Ru^{II}TPPCO) show rapid singlet energy transfer from porphyrin to C₆₀ in solution.⁶ Binuclear (ZnOEP)₂·BPy and (Mn^{II}TPP)₂·DMP assemblies were cocrystallized with (TDAE⁺)·(C₆₀[−]) or (DMETEP⁺)·(C₆₀[−]), respectively (TDAE is tetrakis(dimethylamino)ethylene; DMETEP⁺ is the cation of *N,N'*-dimethyl-*N'*-ethylthioethylpiperazine, Chart 1).^{12,14}

Octaazacryptand (OAC, Chart 1)^{16,17} forms stable inner-sphere complexes with d- and f-metal cations.^{18,19} A free OAC molecule also has six nitrogen atoms accessible for outer-sphere coordination. However, such assemblies were still not obtained. In this work we for the first time used an OAC ligand to prepare coordination assemblies with metalloporphyrins. It has an unusual trinuclear structure and contains manganese(II) tetraphenylporphyrin (Mn^{II}TPP), whose coordination assemblies are rare. By our knowledge, only a binuclear (Mn^{II}TPP)₂·DMP assembly was found in the complex with C₆₀.¹² In our case, the stabilization of (Mn^{II}TPP)₃·OAC in the solid state becomes possible due to the complex formation with fullerene C₇₀: {(Mn^{II}TPP)₃·OAC}·(C₇₀)₃·(C₆H₄Cl₂)₃ (**1**). The IR, UV–vis–NIR, and EPR spectra of **1** were studied to show the neutral ground state and high-spin state of Mn^{II}TPP.

Chart 1



Crystals of {(Mn^{II}TPP)₃·OAC}·(C₇₀)₃·(C₆H₄Cl₂)₃ (**1**) were obtained by diffusion of hexane into a *o*-dichlorobenzene solution containing C₇₀, Mn^{II}TPP, and OAC in anaerobic conditions (Supporting Information). After one month the solvent was decanted and crystals were washed with hexane. The composition of **1** was determined from X-ray diffraction on a single crystal. Several single crystals tested from the synthesis have the same unit cell parameters. The composition of **1** was tested additionally by energy dispersive X-ray analysis (EDX) using an SUPRA-50UP electron microscope to show that the Cl to Mn ratio in the crystals is close to 2:1, in accordance with the composition determined from X-ray diffraction on a single crystal.

The crystal structure of **1** studied at 100(2) K has a high-symmetry hexagonal unit cell.²⁰ Mn^{II}TPP molecules are ordered in this crystal structure. C₇₀ molecules are disordered between two orientations with the 0.679(5)/0.321(5) occupancies. Coordinated OAC molecules are disordered between two positions which shifted relative to each other by the distance between two imine nitrogen atoms of OAC with the 0.679(5)/0.321(5) occupancies. Figures 1, 2d, and 3 show only the major occupied orientations of C₇₀ and OAC molecules. There are three positions of solvent molecules. One solvent molecule occupies positions above and below the coordinated OAC molecule, whereas two other solvent molecules are located in large through channels passing along the *c*-axis. Solvent molecules are strongly disordered in these positions.

*Corresponding author. Fax: +007-496-522-18-52. E-mail: konarev@icp.ac.ru.

The main building block of **1** is a triangle consisting of the coordination $(\text{Mn}^{\text{II}}\text{TPP})_3 \cdot \text{OAC}$ assembly which forms van der Waals contacts with three C_{70} molecules through the $\text{Mn}^{\text{II}}\text{TPP}$

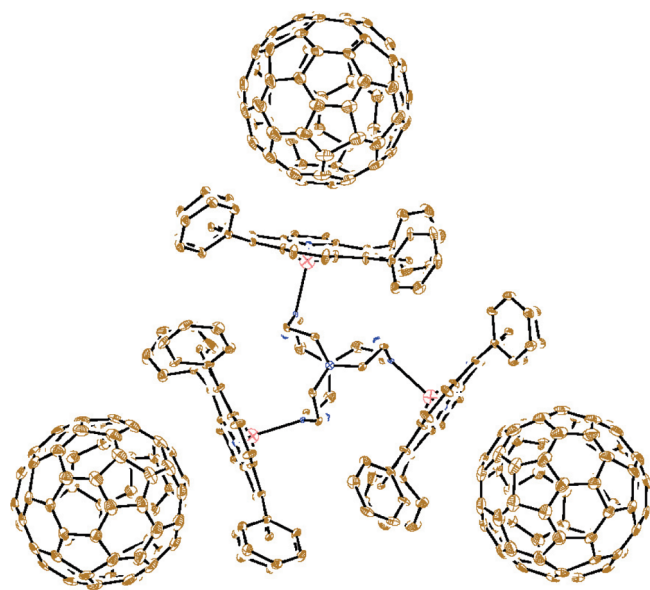


Figure 1. Triangular building block of **1** containing the coordination $(\text{Mn}^{\text{II}}\text{TPP})_3 \cdot \text{OAC}$ assembly (the view along the axis passing through two tertiary nitrogen atoms of OAC) and three C_{70} molecules, which form van der Waals contacts with $\text{Mn}^{\text{II}}\text{TPP}$.

macrocycles (Figure 1). Coordination is realized by imine nitrogen atoms of OAC with the $\text{Mn}^{\text{II}}-\text{N}(\text{OAC})$ distance of 2.283(10) Å. Totally three bulky $\text{Mn}^{\text{II}}\text{TPP}$ molecules coordinate to OAC. Additional coordination of metalloporphyrins is impossible, since the tertiary nitrogen atoms of OAC are not accessible for coordination (they are directed inside the OAC sphere, Figure 2a). Since OAC is asymmetrically positioned relative to the $\text{Mn}^{\text{II}}\text{TPP}$ molecules (Figures 2a and b), free space appears above the coordinated OAC molecules. This space is occupied by solvent molecules (is shown by an oval in Figure 2a). The disorder of OAC is observed due to the fact that it can coordinate to $\text{Mn}^{\text{II}}\text{TPP}$ in two different ways (Figure 2a and c). OAC coordinated to $\text{Mn}^{\text{II}}\text{TPP}$ by another imine nitrogen atom is shifted by the distance between two nitrogen atoms in OAC and has 32.1% occupation. In this case solvent molecules are positioned from the opposite side of OAC (Figure 2c). The mutual orientation of $\text{Mn}^{\text{II}}\text{TPP}$ and C_{70} molecules is depicted in Figure 2d. The Mn^{II} atoms are displaced by 0.507 Å from the plane of four porphyrin nitrogen atoms toward OAC (from the 24-atom porphyrin plane by 0.647 Å), providing the formation of a concave porphyrin surface, corresponding well to the shape of an elongated C_{70} sphere. The shortest van der Waals (VdW) contacts between $\text{Mn}^{\text{II}}\text{TPP}$ and C_{70} are formed mainly with the 6–5 bond of C_{70} (the Mn and $\text{N} \cdots \text{C}(\text{C}_{70})$ distances are in the 3.41–3.48 and 3.19–3.21 Å ranges, respectively). There are also several shortened $\text{C}(\text{Mn}^{\text{II}}\text{TPP}) \cdots \text{C}(\text{C}_{70})$ contacts (Figure 2d).

On the whole, the structure of **1** can be considered as layers arranged in the *ab* plane, which consist of triangles formed by C_{70} molecules and $(\text{Mn}^{\text{II}}\text{TPP})_3 \cdot \text{OAC}$ units held together by van der Waals forces (Figure 3a). Each C_{70} in a triangle forms van der

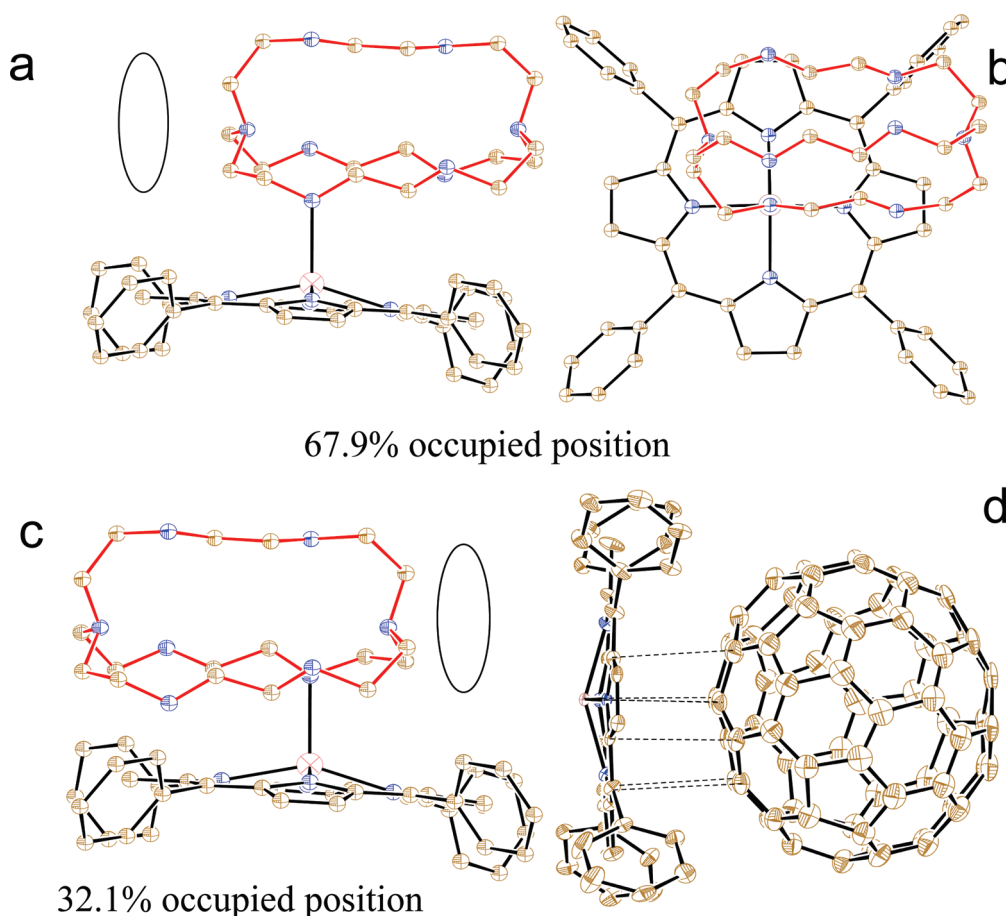


Figure 2. Coordination of OAC to $\text{Mn}^{\text{II}}\text{TPP}$ in the major occupied OAC orientation: the view along the porphyrin plane (a) and the coordination $\text{N}(\text{OAC})-\text{Mn}^{\text{II}}$ bond (b). The coordination of OAC to $\text{Mn}^{\text{II}}\text{TPP}$ in the minor occupied OAC orientation (c). The OAC molecules are shown in red; the position of solvent molecules is shown by ovals. (d) van der Waals contacts between $\text{Mn}^{\text{II}}\text{TPP}$ and C_{70} (dashed lines).

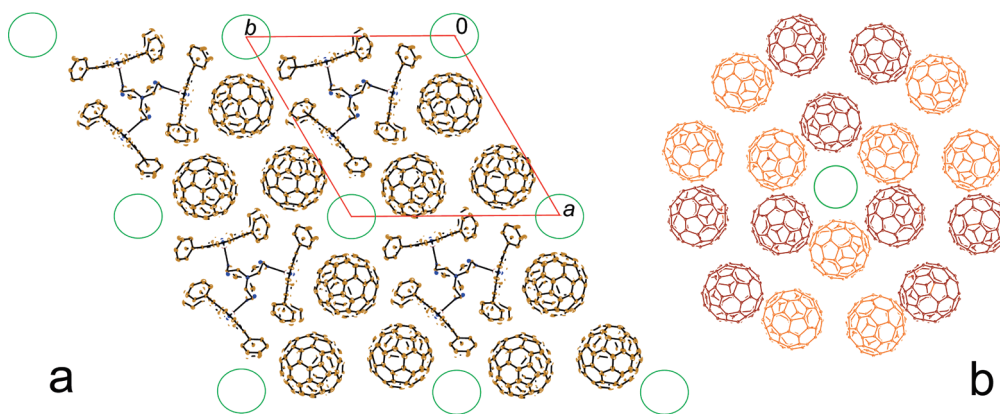


Figure 3. Crystal structure of **1** viewed along the *c*-axis: (a) the layer formed by $(\text{Mn}^{\text{II}}\text{TPP})_3 \cdot \text{OAC}$ and C_{70} triangles; (b) the projection of one fullerene layer onto another (layers are shown by different colors). Green circles show through channels occupied by disordered solvent molecules.

Waals contacts with the porphyrin plane of $\text{Mn}^{\text{II}}\text{TPP}$ and with four phenyl substituents of two other $\text{Mn}^{\text{II}}\text{TPP}$ molecules belonging to the neighboring $(\text{Mn}^{\text{II}}\text{TPP})_3 \cdot \text{OAC}$ units (Figures 2d and 3). The C_{70} molecules are closely packed in triangles with the 10.056 Å distance between the center of mass and form several $\text{C} \cdots \text{C}$ contacts in the 3.32–3.38 Å range with the neighboring C_{70} . Different molecular complexes with fullerene C_{70} were obtained by now.^{21–24} However, such triangular packing of the C_{70} molecules is observed for the first time. The neighboring layers are shifted in such a way that C_{70} triangles lie over the $(\text{Mn}^{\text{II}}\text{TPP})_3 \cdot \text{OAC}$ units from the neighboring layers. As a result of such an arrangement, C_{70} molecules form 3D hexagonal packing with large through channels passing along the *c* axis (Figure 3a and b). These channels are occupied by disordered solvent molecules (green circles in Figure 3a and b). However, there are no short VdW $\text{C} \cdots \text{C}$ contacts between C_{70} molecules from the neighboring layers (the shortest distance between the centers of mass of these fullerenes are 14.3 Å).

The averaged $\text{N}(\text{TPP})\text{--Mn}^{\text{II}}$ bond length of 2.126(4) Å indicates that $\text{Mn}^{\text{II}}\text{TPP}$ has a high ($S = 5/2$) spin state. Five-coordinated high-spin $\text{Mn}^{\text{II}}\text{TPP}$ molecules involved in mono- and binuclear coordination assemblies have similar geometric parameters. For example, $\text{Mn}^{\text{II}}\text{TPP} \cdot \text{Im}$ (Im: *N*-methylimidazole) was characterized by the averaged $\text{N}(\text{TPP})\text{--Mn}^{\text{II}}$ bond lengths of 2.128(2) Å and the displacement of the Mn^{II} atom from the plane of four nitrogen atoms by 0.512 Å (by 0.557 Å from the 24-atom porphyrin plane).²⁵ The averaged $\text{N}(\text{TPP})\text{--Mn}^{\text{II}}$ bond length is 2.141(3) Å for the binuclear $(\text{Mn}^{\text{II}}\text{TPP})_2 \cdot \text{DMP}$ assembly. The displacement of the Mn^{II} atom from the plane of four nitrogen atoms is 0.563 Å (0.677 Å from the 24-atom porphyrin plane).¹⁰

IR and UV–visible–NIR spectra were measured in KBr pellets (Supporting Information). C_{70} shows ten IR-active absorption bands which are not shifted relative to parent C_{70} . The spectrum in the NIR range also indicates the absence of absorption bands in the 800–1200 nm range characteristic of the $\text{C}_{70}^{\cdot -}$ radical anion. Therefore, charge transfer (CT) is absent in the ground state of this complex. Similarly, the degree of CT is close to zero in the C_{70} complex with ligand free $\text{Mn}^{\text{II}}\text{TPP}$.^{22,26} The Soret and Q-bands of $\text{Mn}^{\text{II}}\text{TPP}$ are positioned in the spectrum of **1** at 448 and 572, 612 nm. The positions of these bands in the spectrum of parent $\text{Mn}^{\text{II}}\text{TPP}$ are at 444 and 573, 613 nm. The small shift of the Soret and Q-bands of $\text{Mn}^{\text{II}}\text{TPP}$ can be due to the OAC coordination. A weak broad band in the spectrum of **1** near 820 nm was attributed to CT at the absorption of a light quantum. It is interesting that different C_{60} complexes with ZnTPP assemblies also manifest CT bands at 760–820 nm.¹⁰ $\text{Mn}^{\text{II}}\text{TPP}$ is a rather strong donor in polar solvents. The first oxidation potential of $\text{Mn}^{\text{II}}\text{TPP}$ in acetonitrile is -0.23 V vs SCE,²⁷ whereas the first reduction potential of C_{70} in dichloromethane is -0.41 V vs

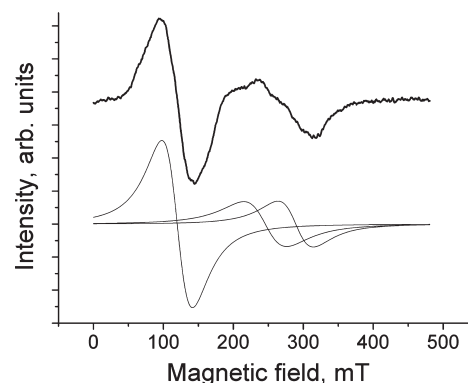


Figure 4. Room-temperature EPR spectrum of polycrystalline **1**. The fitting of the spectrum by three Lorentzian lines is shown at the bottom (the *g*-factors of the lines are given in the text).

SCE.²⁸ ZnTPP is oxidized at essentially higher potentials ($+0.79$ V vs SCE in benzonitrile).²⁹ However, the position of the CT band in the solid state for a series of complexes with one acceptor is determined by the vertical ionization potentials of the donors in a gas phase.³⁰ $\text{Mn}^{\text{II}}\text{TPP}$ and ZnTPP have close vertical ionization potentials (6.42 and 6.44 eV, respectively),³¹ providing close CT energies in the complexes of these porphyrins with fullerenes.

Ligand free high-spin ($S = 5/2$) $\text{Mn}^{\text{II}}\text{TPP}$ shows an anisotropic EPR spectrum ($g_{\perp} = 5.9$, $g_{\parallel} = 2.0$) with a hyperfine structure (HFS) due to the interaction between the unpaired electron and the ^{55}Mn nucleus ($I = 5/2$).³² The EPR spectrum of **1** also shows a signal at low magnetic fields ($g_1 = 5.618$) expected for high-spin $\text{Mn}^{\text{II}}\text{TPP}$. As a whole, the signal is strongly asymmetric and can be well fitted by three Lorentzian lines with $g_1 = 5.618$, $g_2 = 2.738$, and $g_3 = 2.326$ (Figure 4).

We obtained a trinuclear coordination $(\text{Mn}^{\text{II}}\text{TPP})_3 \cdot \text{OAC}$ assembly of manganese(II) tetraphenylporphyrins with octaaza-cryptand stabilized in the solid state by complex formation with fullerene C_{70} . Without fullerene we could not prepare crystals of $(\text{Mn}^{\text{II}}\text{TPP})_3 \cdot \text{OAC}$ suitable for the X-ray diffraction experiment. Therefore, it is not possible to suppose what structure is formed without fullerene. A trinuclear metalloporphyrin assembly was only found for the (4-pyridyl)triazine bridging ligand with ruthenium(II) porphyrin,³³ whereas such an assembly with $\text{Mn}^{\text{II}}\text{TPP}$ was obtained for the first time. Only three $\text{Mn}^{\text{II}}\text{TPP}$ can coordinate to OAC due to steric reasons, but we can expect the formation of coordination structures when only one or two metalloporphyrin molecules coordinate to OAC. The geometric parameters for $\text{Mn}^{\text{II}}\text{TPP}$ are the evidence of its high-spin ($S = 5/2$) state, which was proved by the EPR spectrum of **1**. The

porphyrin macrocycle forms a concave surface due to the coordination of OAC to Mn^{II}TPP. Such a surface conforms well to the ellipsoidal C₇₀ shape and provides the appearance of a rather intense CT band in the visible–NIR spectrum of **1**. Nevertheless, IR, visible–NIR, and EPR spectra of **1** indicate a neutral ground state of the complex. The position of the CT band in the spectrum of **1** is close to those in the spectra of molecular C₆₀ complexes with ZnTPP·L assemblies.¹⁰ The possible reason for that is the close vertical ionization potentials of Mn^{II}TPP and ZnTPP.

Acknowledgment. This work was supported by RFBR Grant No. 09-02-01514.

Supporting Information Available: X-ray crystallographic information file (CIF) for complex **1**, experimental section, IR data for the starting compounds and complex **1**, and UV–visible–NIR spectrum of Mn^{II}TPP and complex **1**. This material is available free of charge via the Internet at <http://pubs.acs.org>.

References

- (1) Goldberg, I. *CrystEngComm* **2002**, *4*, 109–116.
- (2) Bouamaied, I.; Coskun, T.; Stulz, E. *Struct. Bonding (Berlin)* **2006**, *121*, 1–47.
- (3) Shukla, A. D.; Dave, P. C.; Surech, E.; Das, A.; Dastidar, P. *J. Chem. Soc., Dalton. Trans* **2000**, 4459–4463.
- (4) Kumar, R. K.; Diskin-Posner, Y.; Goldberg, I. *J. Inclusion Phenom. Macrocyclic Chem.* **2000**, *37*, 219–230.
- (5) Kumar, R. K.; Goldberg, I. *Angew. Chem., Int. Ed.* **1998**, *37*, 3027–3030.
- (6) Guldi, D. M.; Da Ros, T.; Braiuca, P.; Prato, M.; Alessio, E. *J. Mater. Chem.* **2002**, *12*, 2001–2008.
- (7) Gust, D.; Moore, T. A.; Moore, A. L. *Acc. Chem. Res.* **2001**, *34*, 40–48.
- (8) Hajjaj, F.; Yoon, Z. S.; Yoon, M.-C.; Park, J.; Satake, A.; Kim, D.; Kobuke, Y. *J. Am. Chem. Soc.* **2006**, *128*, 4612–4623.
- (9) Konarev, D. V.; Kovalevsky, A. Yu.; Li, X.; Neretin, I. S.; Litvinov, A. L.; Drichko, N. V.; Slovokhotov, Yu. L.; Coppens, P.; Lyubovskaya, R. N. *Inorg. Chem.* **2002**, *41*, 3638–3646.
- (10) Litvinov, A. L.; Konarev, D. V.; Kovalevsky, A. Yu.; Coppens, P.; Lyubovskaya, R. N. *Cryst. Growth Des.* **2005**, *5*, 1807–1819.
- (11) Litvinov, A. L.; Konarev, D. V.; Kovalevsky, A. Yu.; Coppens, P.; Lyubovskaya, R. N. *CrystEngComm* **2003**, *5*, 137–139.
- (12) Konarev, D. V.; Khasanov, S. S.; Saito, G.; Otsuka, A.; Lyubovskaya, R. N. *Inorg. Chem.* **2007**, *46*, 7601–7609.
- (13) Konarev, D. V.; Neretin, I. S.; Litvinov, A. L.; Drichko, N. V.; Slovokhotov, Yu. L.; Lyubovskaya, R. N.; Howard, J. A. K.; Yufit, D. S. *Cryst. Growth Des.* **2004**, *4*, 643–646.
- (14) Konarev, D. V.; Khasanov, S. S.; Slovokhotov, Yu. L.; Saito, G.; Lyubovskaya, R. N. *CrystEngComm* **2008**, *10*, 48–53.
- (15) Konarev, D. V.; Khasanov, S. S.; Saito, G.; Lyubovskaya, R. N. *Cryst. Growth Des.* **2009**, *9*, 1170–1181.
- (16) Smith, P. H.; Barr, M. E.; Brainard, J. R.; Ford, D. K.; Frieser, H.; Muralidharar, S.; Reilly, S. D.; Ryan, R. R.; Selles, L. A.; Yu., W. H. *J. Org. Chem.* **1993**, *58*, 7939–7941.
- (17) McKee, J.; Nelson, J. *Acta Crystallogr.* **1999**, *C55*, 1494–1496.
- (18) Hanter, L.; Nelson, J.; Harding, C. L.; McKee, V.; McCann, M. *J. Chem. Soc., Chem. Commun.* **1990**, 1148–1151.
- (19) Blingh, S. W. A.; Drew, M. G. B.; Martin, N.; Maubert, B.; Nelson, J. *J. Chem. Soc., Dalton Trans.* **1998**, 3711–3713.
- (20) Crystal data of **1** at 100(2) K: C₃₇₈H₁₂₆N₂₀Cl₆Mn₃, *M_r* = 5324.52 g · mol^{−1}, black, hexagonal, *P*₆₃, *a* = 23.6415(9), *b* = 23.6415(9), *c* = 23.7812(13) Å, *V* = 11511.0(9) Å³, *Z* = 2, *d*_{calc} = 1.536 g · cm^{−3}, *μ* = 0.312 mm^{−1}, data/parameters 2676/1654, *R*₁ = 0.0900 [*I* > 2σ(*I*)], *wR*₂ = 0.2749, GOF = 1.051. CCDC reference is 742741.
- (21) Olmstead, M. M.; Costa, D. A.; Maitra, K.; Noll, B. C.; Phillips, S. L.; Van Calcar, P. M.; Balch, A. L. *J. Am. Chem. Soc.* **1999**, *121*, 7090–7097.
- (22) Konarev, D. V.; Neretin, I. S.; Slovokhotov, Yu. L.; Yudanov, E. I.; Drichko, N. V.; Shulga, Yu. M.; Tarasov, B. P.; Gumanov, L. L.; Batsanov, A. S.; Howard, J. A. K.; Lyubovskaya, R. N. *Chem.—Eur. J.* **2001**, *7*, 2605–2616.
- (23) Makha, M.; Raston, C. L.; Sobolev, A. N.; Turner, P. *Cryst. Growth. Des.* **2006**, *6*, 224–228.
- (24) Makha, M.; Scott, J. L.; Strauss, C. R.; Sobolev, A. N.; Raston, C. L. *Cryst. Growth. Des.* **2009**, *9*, 483–487.
- (25) Kirner, J. F.; Reed, C. A.; Scheidt, W. R. *J. Am. Chem. Soc.* **1977**, *99*, 2557–2563.
- (26) Yudanov, E. I.; Konarev, D. V.; Gumanov, L. L.; Lyubovskaya, R. N. *Russ. Chem. Bull.* **1999**, *48*, 718–721.
- (27) Nagai, K.; Iyoda, T.; Hashimoto, K.; Fujishima, A. Abstr. Int. Conf. Perspectives in Organic–Inorganic Hybrid Solids, Nagoya, Japan, 1996; p 118.
- (28) Dubois, D.; Kadish, K. M.; Flanagan, S.; Haufler, R. F.; Chibante, L. P. F.; Wilson, L. J. *J. Am. Chem. Soc.* **1991**, *113*, 4364–4366.
- (29) Wolberg, A.; Manassen, J. *J. Am. Chem. Soc.* **1970**, *92*, 2982–2991.
- (30) Mulliken, R. S.; Person, W. B. *Molecular Complexes*; Academic Press: New York, 1969.
- (31) Khandelwal, S. C.; Roebber, J. L. *Chem. Phys. Lett.* **1975**, *34*, 355–359.
- (32) Hoffman, B. M.; Weschler, C. J.; Basolo, F. *J. Am. Chem. Soc.* **1976**, *98*, 5473–5482.
- (33) Darling, S. L.; Mac, C. C.; Bampos, N.; Feeder, N.; Teat, S. J.; Sanders, J. K. M. *New J. Chem.* **1999**, *23*, 359–364.